Dyes and Pigments 86 (2010) 107–114

Contents lists available at ScienceDirect

Dyes and Pigments

journal homepage: www.elsevier.com/locate/dyepig

The synthesis and optical properties of novel fluorinated polyimides incorporated with highly electro-optic active thiazole and benzothiazole based chromophores

Man He [a], Yuming Zhou [a,*], Junliang Miao [a], Cheng Liu [a], Yiping Cui [b], Tong Zhang [b]

[a] School of Chemistry and Chemical Engineering, Southeast University, Nanjing 211189, China
[b] Department of Electronic Engineering, Southeast University, Nanjing 210096, China

A R T I C L E I N F O

Article history:
Received 12 July 2009
Received in revised form
28 November 2009
Accepted 30 November 2009
Available online 16 December 2009

Keywords:
Polyimides
Hetarylazo chromophores
NLO
Side-chain
Optical loss
Stability

A B S T R A C T

Novel, non-linear optical fluorinated polyimides were prepared by the Mitsunobu reaction of hydroxyl-containing hetarylazo chromophores with hydroxyl polyimides. Their structures were verified by FT-IR, ^{1}H NMR, UV–Vis spectra, elemental analysis and gel permeation chromatography. The resulting amorphous polyimides exhibited good solubility and can be easily spin-coated into thin films with good optical quality. The high electro-optic coefficients (r_{33}) obtained for the films of poled polyimides were attributed to the introduction of hetarylazo chromophores with large hyperpolarizability within the polyimides. The polyimides possess high glass transition temperature (201–210 °C) and therefore showed excellent temporal stability, retaining 88% of their initial non-linear optical response at 110 °C for >200 h. Low optical losses in the range of 1.9–2.3 dB cm^{-1} at 1550 nm were observed for the polyimides and the values of thermooptic coefficients ranged from -1.680×10^{-4} to -2.008×10^{-4}/°C.

1. Introduction

Polymeric materials with second-order NLO properties have attracted much interest in recent years as promising candidates for application in electro-optic and photonic devices. For practical applications, such NLO polymeric materials must display good film-forming properties, sufficiently large and stable NLO susceptibility, low optical propagation loss, high thermal stability and satisfactory processability. Although it is extremely difficult to synthesize materials which possess all of these properties, large and thermally stable EO activity and low optical loss are particularly required for device application.

Aromatic polyimides have been shown to offer a means of preventing relaxation of poled order in poled polymers owing to their high glass transition temperature. Various polyimide-based NLO materials exhibiting high-temperature alignment stability, high T_g and thermal stability have been developed [1–22]. The present authors have prepared a series of side-chain polyimides second-order NLO materials comprising azo chromophores in the past years [23]; however optical losses at 1.55 μm telecommunication wavelength were not measured. An important property of the side-chain polyimides prepared in this work was low optical loss at the 1.55 μm telecommunication wavelength. In addition, as the rigid backbone of aromatic polyimides can result in poor solubility and undesirable film formation quality, a fluorinated moiety was introduced into the polyimide backbone to increase solubility and processability. Moreover, C–F overtones have extremely low absorption in the telecommunications window, owing to their higher harmonic order and fluorinated polyimides are known to reduce propagation loss because of their high optical transparency at these particular wavelengths.

It is known that large NLO responses are indispensable for the realization of EO devices. As chromophores could play the role of NLO elements in polymeric systems, the design and synthesis of chromophores with large hyperpolarizability is very important in the development of NLO devices. Theoretical NLO studies have revealed that heteroaromatic rings play a subtle role in influence the second-order NLO properties of push–pull chromophores [24–30]. Replacing the benzene ring of a chromophore bridge with heteroaromatic rings, such as thiazole and benzothiazole, can results in an increased molecular hyperpolarizability. Thus, in recent papers some hetarylazo chromophores distinguished by large hyperpolarizability for non-linear optical application have been synthesized by our group [31,32]. The use of highly electro-optic active hetarylazo chromophores in the fluorinated polyimides is expected to result in a high-performance polymeric system. In addition, up to now we note that azo chromophores with heteroaromatic rings have been mainly employed in guest–host systems,

---

* Corresponding author. Tel/fax: +86 25 52090617.
E-mail address: fchem@seu.edu.cn (Y. Zhou).

0143-7208/$ – see front matter © 2010 Elsevier Ltd. All rights reserved.
doi:10.1016/j.dyepig.2009.11.008

while very few examples of side-chain polyimides have been reported. This paper reports our efforts to extend our previous work in order to incorporate the hetarylazo chromophores to the fluorinated polyimide matrixes to obtain novel NLO side-chain fluorinated polyimides. The side-chain polyimides with hetarylazo chromophores show a large second-order optical nonlinearity. Therefore the new fluorinated polyimides with NLO hetarylazo chromophores are distinguished by an excellent combination of high glass transition temperature, processibility, large NLO activity, long-term stability and low optical loss. And these desirable properties provide great promise in the development of EO devices.

2. Experimental

2.1. Materials

N,N-Dimethylformamide (DMF) was stirred over powered calcium hydride overnight and then distilled under reduced pressure. Cyclopentanone and tetrahydrofuran (THF) were purified by distillation and other regents and solvents were analytically pure and used without further purification. The monomers 4,4′-(hexafluoroisopropylidene) diphthalicanhydride (6FDA) and 2,2′-bis(3-amino-4-hydroxy-phenyl) hexafluoropropane (6FHP) were obtained from Tokyo Chemical Industry (TCI) and were used without further purification. 2-[4′-(N-Ethyl-N-2-hydroxyethyl)-amino-phenylazo]-6-nitrobenzothiazole (EHNBT) and 2-[4′-(N-Ethyl-N-2-hydroxyethyl)-amino-phenylazo]-5-nitrothiazole (EHNT) were prepared according to the literature [24,31].

2.2. Instrumentation

^{1}H NMR spectra were recorded with the use of a Bruker 300 MHz spectrometer using dimethyl sulphoxide (DMSO) as solvent and tetramethyl silane (TMS) as internal standard. FT-IR spectra were measured as KBr pellets on a Nicolet 750 series in the region of 4000–400 cm^{-1}. UV–Vis absorption spectra were measured on a Shimadzu UV 2201 spectrometer. Elemental analysis was obtained using a Perkin–Elmer Lambda 6 elemental analyzer. Thermogravimetric analysis (TGA) and differential scanning calorimetry (DSC) were performed on NETZSCH STA449C under a nitrogen atmosphere at the heating rate of 10 °C/min. Molecular weights were determined by GPC with a polystyrene standard using a WATERS SEC-244 system at 25.5 °C in THF.

2.3. Synthesis of side-chain NLO polyimides

Synthesis of side-chain NLO polyimides was carried out by the Mitsunobu reaction of hydroxy-containing polyimides with NLO chromophores, as shown in Fig. 1.

2.3.1. Synthesis of hydroxy-containing polyimide FPI based on 6FHP and 6FDA

Polymerization was conducted in a dry nitrogen-flushed, three-neck flask equipped with a magnetic stirrer. 6FDA (1.33 g, 3 mmol) was completely dissolved in 8 mL DMF, and 6FHP (1.10 g, 3 mmol) in 6 mL DMF was added at 0 °C. The solution was warmed to room temperature and magnetically stirred overnight under nitrogen to realise the poly(amic acid) solution. The viscosity of the solution increased during this period greatly. Dry xylene (8 mL) was added and the ensuing poly(amic acid) was thermally cyclized in an oil bath at 160 °C for 5 h under nitrogen. The resulting solution was added dropwise to a solution of 1:1 methanol:water solution (50 mL) and 2 M aq HCl solution (10 mL) in a high-speed blender to obtain the yellow hydroxy-containing polyimide. The polymer was redissolved in THF, and further reprecipitated into a solution of methanol/water (1:1). The product was collected by filtration, washed by above solution for three times, and dried at 60 °C under vacuum for 24 h.

2.3.2. Synthesis of hydroxy-containing polyimide PFPI based on 6FHP, pyromellitic dianhydride (PMDA) and 6FDA

PMDA (0.65 g, 3 mmol) and 6FDA (1.33 g, 3 mmol) were completely dissolved in 9 mL DMF and 6FHP (2.20 g, 6 mmol) in 8 mL DMF was added to the mixed DMF solution at 0 °C. The solution was warmed to room temperature and magnetically stirred overnight under nitrogen to form the poly(amic acid) solution. The viscosity of the solution increased during this period greatly. Dry xylene (16 mL) was added to the flask, and the poly (amic acid) was thermally cyclized in an oil bath at 160 °C for 5 h under nitrogen atmosphere. The resulting solution was added dropwise into a solution of 1:1 methanol/water solution (50 mL) and 2 M aq HCl solution (10 mL) in a high-speed blender to obtain the yellow hydroxy-containing polyimide. The polymer was redissolved in THF, and further reprecipitated into a solution of methanol/water (1:1). The product was collected by filtration, washed by above solution for three times, and dried at 60 °C under vacuum for 24 h.

2.3.3. Synthesis of side-chain polyimides FPI-EHNT, FPI-EHNBT, PFPI-EHNT and PFPI-EHNBT

A general procedure for the synthesis of side-chain polyimides FPI-EHNT, FPI-EHNBT, PFPI-EHNT and PFPI-EHNBT is as follows. 0.61 g of the hydroxy-containing polyimide FPI, EHNT (0.50 g, 1.57 mmol) and triphenylphosphorus (PPh$_3$: caution - incompatible with oxidizing agents, acids; 0.62 g, 2.35 mmol) were dissolved in dry THF (15 mL) successively. Diethyl azodicarboxylate (DEAD) (0.41 g, 2.35 mmol) was added dropwise to the solution under nitrogen atmosphere. The reaction mixture was stirred for two days at room temperature, and then the resulting reaction solution was added dropwise into an agitated solution of methanol/water (1:1, 200 mL) and 2 N HCl (1 mL) in a high-speed blender. The collected solid was dissolved in THF and then precipitated into the solution of methanol/water. The product FPI-EHNT was filtered out and washed with methanol/water for several times, and dried at 60 °C under vacuum for 24 h. IR (KBr, cm^{-1}): 1790 (m, C = O), 1730 (vs, C = O), 1380 (m, CN), 1340 (s, N = O), 723 (s, imide ring). ^{1}H NMR (DMSO-d$_6$, ppm): δ = 1.21 (t, $-CH_2C\mathbf{H_3}$, 6H), 3.65 (t, $-C\mathbf{H_2}-$, 12H), 7.04 (d, Ar-**H**, 4H), 7.17 (d, Ar-**H**, 2H), 7.36 (d, Ar-**H**, 2H), 7.49 (s, Ar-**H**, 2H), 7.70 (s, Ar-**H**, 2H), 7.82 (d, Ar-**H**, 4H), 8.06–8.13 (m, Ar-**H**, 4H), 8.79 (s, Ar-**H**, 2H). Anal. calcd for $C_{47}H_{26}F_{12}N_7O_8S$ (1076.60): C, 52.44%; H, 2.42%; N, 9.11%; S, 2.98%. Found: C, 52.30%; H, 2.25%; N, 9.31%; S, 3.05%.

The side-chain polyimide FPI-EHNBT was synthesized by a procedure similar to that for polymide FPI-EHNT by using chromophore EHNBT instead of EHNT. FPI-EHNBT IR (KBr, cm^{-1}): 1790 (m, C = O), 1730 (vs, C = O), 1380 (m, CN), 1340 (s, N = O), 723 (s, imide ring). ^{1}H NMR (DMSO-d$_6$, ppm): δ = 1.20 (m, $-CH_2C\mathbf{H_3}$, 6H), 3.65 (t, $-C\mathbf{H_2}-$, 12H), 6.99 (d, Ar-**H**, 4H), 7.17 (d, Ar-**H**, 2H), 7.36 (d, Ar-**H**, 2H), 7.49 (s, Ar-**H**, 2H), 7.70 (s, Ar-**H**, 2H), 7.85 (d, Ar-**H**, 4H), 8.06–8.13 (m, Ar-**H**, 6H), 8.29 (q, Ar-**H**, 2H), 8.99 (d, Ar-**H**, 2H). Anal. calcd for $C_{51}H_{28}F_{12}N_7O_8S$ (1126.64): C, 54.37%; H, 2.49%; N, 8.70%; S, 2.85%. Found: C, 54.21%; H, 2.28%; N, 8.90%; S, 2.70%.

Side-chain polyimide PFPI-EHNT was synthesized by a procedure similar to that for polymide FPI-EHNT by using hydroxy-containing polyimide PFPI instead of FPI. PFPI-EHNT IR (KBr, cm^{-1}): 1780 (m, C = O), 1730 (vs, C = O), 1380 (m, CN), 1340 (s, N = O), 723 (s, imide ring). ^{1}H NMR (DMSO-d$_6$, ppm): δ = 1.20 (t, $-CH_2C\mathbf{H_3}$, 12H), 3.65 (t, $-C\mathbf{H_2}-$, 24H), 7.04 (d, Ar-**H**, 8H), 7.17 (d, Ar-**H**, 4H), 7.36 (d, Ar-**H**, 4H), 7.49 (s, Ar-**H**, 4H), 7.70 (s, Ar-**H**, 2H), 7.82 (d, Ar-**H**, 8H), 8.06–8.13 (m, Ar-**H**, 4H), 8.79 (s, Ar-**H**, 4H), 9.00 (s, Ar-**H**, 2H).

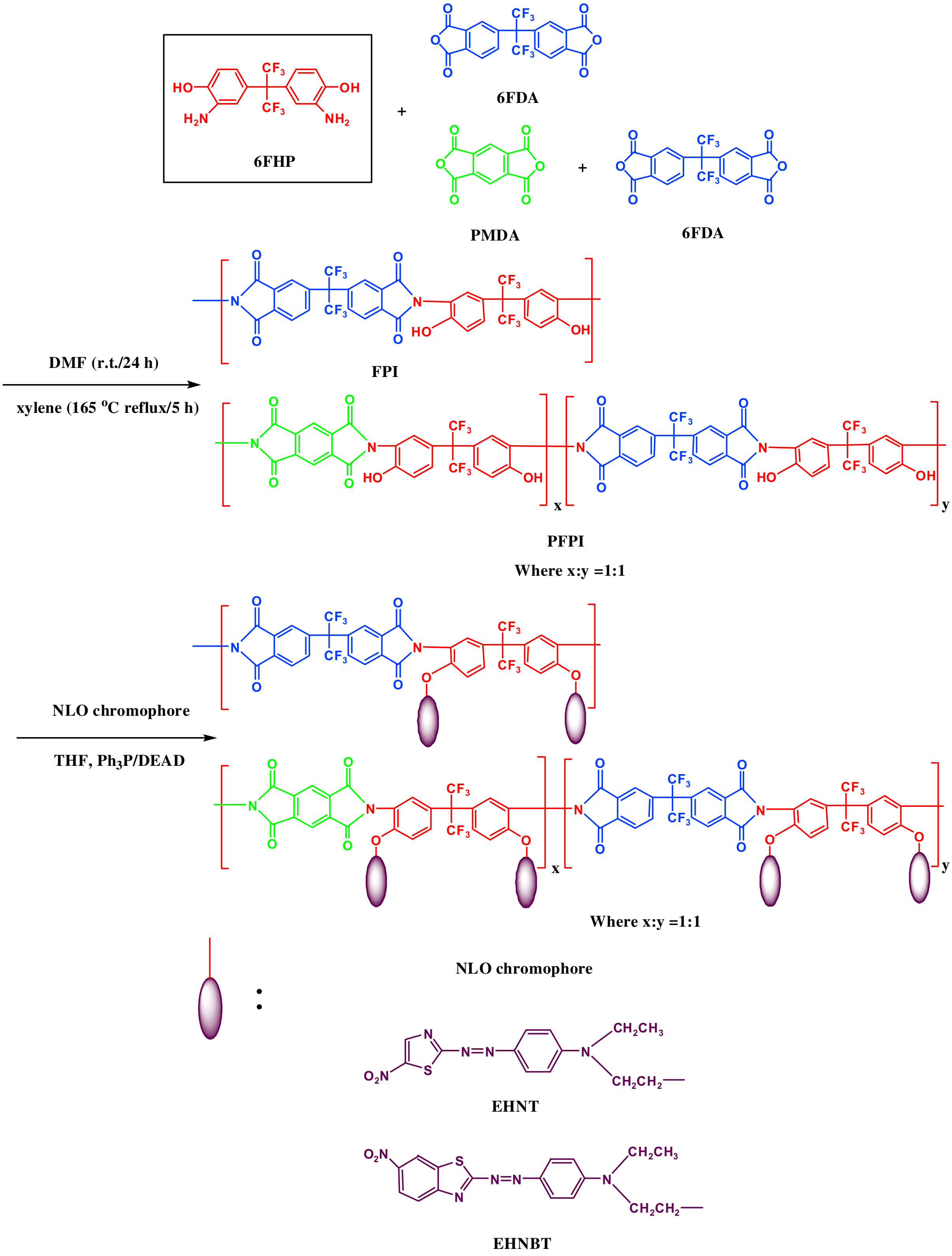

Fig. 1. Synthesis of the side-chain NLO polyimides by Mitsunobu reaction.

Anal. calcd for $C_{72}H_{34}F_{18}N_9O_{14}S$(1622.87): C, 53.29%; H, 2.10%; N, 7.77%; S, 1.98%. Found: C, 53.01%; H, 2.34%; N, 7.52%; S, 1.85%.

Side-chain polyimide PFPI-EHNBT was synthesized by a procedure similar to that for polymide FPI-EHNT by using hydroxy-containing polyimide PFPI and chromophore EHNBT instead of hydroxy-containing polyimide FPI and chromophore EHNT, respectively. PFPI-EHNBT IR (KBr, cm^{-1}): 1780 (m, C=O), 1730 (vs, C=O), 1380 (m, CN), 1340 (s, N=O), 721 (s, imide ring).

^{1}H NMR (DMSO-d$_6$, ppm): $\delta = 1.20$ (m, $-\mathrm{CH_2C}\mathbf{H_3}$, 12H), 3.65 (t, $-\mathrm{C}\mathbf{H_2}-$, 24H), 6.99 (d, Ar-**H**, 8H), 7.17 (d, Ar-**H**, 4H), 7.36 (d, Ar-**H**, 4H), 7.49 (s, Ar-**H**, 4H), 7.70 (s, Ar-**H**, 2H), 7.85 (d, Ar-**H**, 8H), 8.06–8.13 (m, Ar-**H**, 4H), 8.29 (q, Ar-**H**, 4H), 8.98–9.00 (m, Ar-**H**, 6H). Anal. calcd for $C_{76}H_{36}F_{18}N_9O_{14}S$(1672.91): C, 54.57%; H, 2.15%; N, 7.54%; S, 1.92%. Found: C, 54.42%; H, 2.33%; N, 7.38%; S, 1.88%.

2.4. Thin film preparation, poling process, EO coefficient and optical loss measurements

The polymers were dissolved in cyclopentanone at a concentration of range of 20–30 wt.%, depending on the desired film thickness. The polymer solution was filtered through a 0.5 μm syringe filter and spin-coated onto indium-tin oxide (ITO) glass substrates, which were carefully pre-cleaned by alcohol, acetone and distilled water sequentially in an ultrasonic bath. After coating, these thin films were dried in vacuum at 60 °C for 24 h to remove residual solvent. The poling process for the second-order NLO polymer films was carried out using a corona poling technique. The poling voltage was maintained for 8 kV and the temperature was kept at approximately 10 °C lower than the T_g of the sample for a certain period of time. The sample was then cooled down to room temperature in the presence of a poling field. EO coefficients of the poled films were measured at 1550 nm using the simple reflection technique. The refractive index, the thickness and optical loss were measured by a Model SPA-4000 Prism Coupler at 1550 nm.

3. Results and discussion

3.1. Synthesis and characterization of the side-chain NLO polyimides

The synthesis of the side-chain NLO polyimides was carried out in a two-step reaction. The first step was for the synthesis of hydroxyl polyimides and the second for the incorporation of the NLO chromophores to the polymer backbone by the Mitsunobu reaction. The molar ratio (x/y) of the hydroxyl polyimide PFPI component refers to the molar ratio of PMDA: 6FDA in the initial monomer feed. The molar ratio (x/y) was readily controlled through the monomer feed ratio of PMDA to 6FDA. The synthetic method is a convenient and easy procedure to obtain the side-chain NLO polyimides. Because of the mild conditions there are no restrictions for the kind of chromophore to be incorporated into the polymer structure. We can easily incorporate many kinds of NLO chromophores (see Fig. 2 for examples) containing hydroxyl group into different polyimide backbones to create various side-chain NLO polyimides. The FT-IR spectra of all side-chain polyimides show clearly characteristic peaks at approximately 1730 cm^{-1} and 1790 cm^{-1} for the symmetric and asymmetric vibration bands of the C=O linkage in the cyclic imide group, respectively. All of these side-chain polyimides exhibit strong absorption at about 1380 cm^{-1} and 723 cm^{-1}, which shows the presence of the imide heterocycle in these polymers. The strong absorption band due to the nitro group in the NLO chromophore appear near 1340 cm^{-1}, clearly indicating the presence of the NLO chromophore in the polyimides. ^{1}H NMR spectra show that the chemical shifts due to NLO chromophores protons do not exhibit much change on going from chromophores to terminal polymers. Hydroxy proton chemical shifts of both the hydroxypolyimide backbone and the chromophore almost disappeared in ^{1}H NMR after the reaction, where the spectral assignments clearly support the proposed structures. The GPC measurement gives the weight-average molecular weights ($\overline{M}_w$) of the side-chain polyimides in the range of 41,560–47,610 with the polydispersities ($\overline{M}_w/\overline{M}_n$) from 2.1 to 2.5.

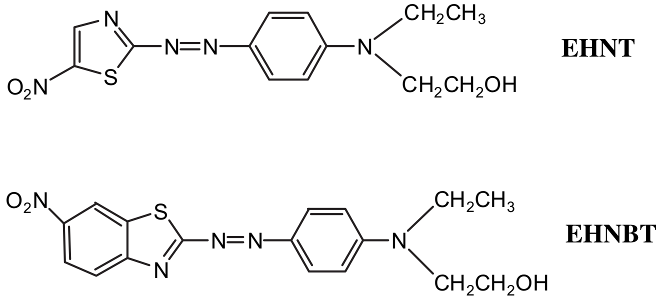

Fig. 2. Chemical structure of the NLO chromophores.

Fig. 3 shows the UV–Vis spectra of the side-chain NLO polyimides and chromophores in the N-methyl-2-pyrrolidone (NMP) solution. Correspondingly, the values of the absorption maxima (λ_{max}) are listed in Table 1. The side-chain NLO polyimides have a maximum absorption wavelength ranging from 565.5 nm to 598 nm, mainly resulting from the intra-molecular charge transfer of the hetarylazo chromophores. The result further confirms that the hetarylazo chromophores were successfully introduced into the side chains of the polyimides. From Table 1, the values of the λ_{max} of the side-chain NLO polyimides indicate that the incorporation of the same chromophore to different polymer backbone results in a small change of the λ_{max}. The UV behavior suggests that the λ_{max} of the side-chain NLO polyimides is affected a little by the stiffness of the polyimide backbone. The λ_{max} of the side-chain NLO polyimides are slightly blue-shifted compared with those of the corresponding hetarylazo chromophores, which indicates the influence of polyimide backbones. The maximum absorption wavelengths of PFPI-EHNT and FPI-EHNT are red-shifted, in comparison with those of PFPI-EHNBT and FPI-EHNBT, due to the enhancement of intra-molecular charge-transferring degree in thiazolylazo chromophore EHNT. However, this large bathochromic shift of the λ_{max} is beneficial to give large NLO response. In addition the deviation of the band edges for the polymers from the operating wavelengths of the laser for telecommunication may help to decrease the absorption optical loss. According to the method described in the literature [4,33], the hetarylazo chromophores content in FPI-EHNT can be estimated. A series of NMP solutions of the chromophore EHNT with concentration in the range of 1×10^{-5}-4×10^{-5} mol/L were prepared and a calibration curve was drawn from their absorption data in UV–Vis spectra at about 601 nm. Then the spectrum of an NMP solution of FPI-EHNT

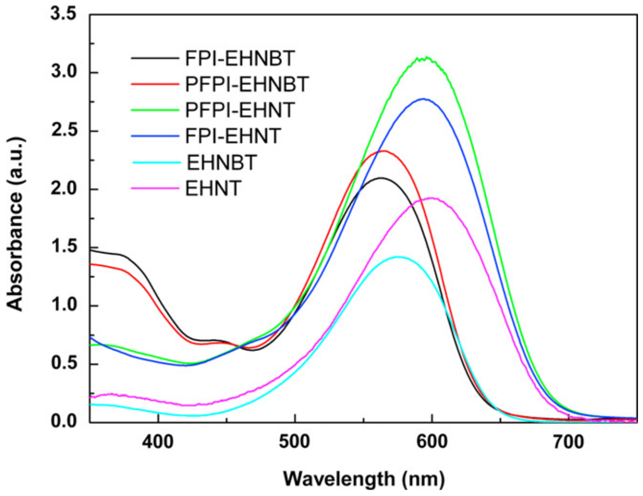

Fig. 3. UV–Vis absorption spectra of NMP solutions of the side-chain polyimides and chromophores.

Table 1
Physical property of the side-chain NLO polyimides.

	$\overline{M}_w$	$\overline{M}_w/\overline{M}_n$	Content (%)[a]	λ_{max} (nm)[b]	T_g (°C)	T_d(°C)
FPI-EHNT	41,560	2.2	43	595.5 (601)	203	242
FPI-EHNBT	43,230	2.1	46	565.5 (575)	201	289
PFPI-EHNT	46,890	2.3	47	598 (601)	210	239
PFPI-EHNBT	47,610	2.5	52	567.5 (575)	208	287

[a] Chromophore-side-chain content (wt/wt) in polymer.
[b] The maximum absorption wavelengths of the hetarylazo chromophores in NMP are given in parentheses.

(0.03 mg/mL) was measured. Using the calibration curve, the azo chromophore content incorporated in FPI-EHNT was calculated to be 43 wt%. Similarly the azo chromophore contents incorporated in other polymers were calculated using a calibration curve obtained with the pure chromophore and the results are shown in Table 1.

3.2. Thermal properties

Thermal properties of the side-chain NLO polyimides were examined by TGA and DSC. The results are summarized in Table 1. DSC analysis showed T_g values in the range between 201 and 210 °C for the side-chain NLO polyimides. The relatively high T_g of the polyimides would make them exhibit good thermal stability of the dipole reorientation in the polymers after poling. Fig. 4 shows the TGA curves of the side-chain NLO polyimides. TGA traces show that these polyimides have decomposition temperatures in the range of 239–289 °C, which represents the decomposition of the NLO chromophores from the polymer backbone. The polyimides FPI-EHNBT and PFPI-EHNBT containing a side-chain benzothiazolylazo chromophore have higher thermal decomposition temperatures than the polyimides FPI-EHNT and PFPI-EHNT, which has a thiazolylazo chromophore as a side-chain. The increase of the thermal stability for the polyimides FPI-EHNBT and PFPI-EHNBT can be attributed to high thermal decomposition temperature of benzothiazolylazo chromophore compared with that of thiazolylazo chromophore. The thermal decomposition temperatures of the side-chain NLO polyimides are higher than the corresponding T_g's and this high thermal stability will ensure high-temperature electric poling of the polymers.

3.3. Linear optical properties

An attempt was made to estimate the crystallinity of the side-chain NLO polyimides by means of X-ray diffraction (XRD) measurement. The typical wide-angle X-ray diffraction pattern of polyimide FPI-EHNT is presented in Fig. 5. In Fig. 5 no obvious diffraction peak observed in XRD diagram reveals the amorphous nature of the side-chain NLO polyimides. This might be interpreted by the presence of bulky trifluoromethyl groups and side-chain chromophores, which decrease the intra- and inter-polymer chain interactions, resulting in loose polymer chain packaging and aggregates. The amorphous samples were obtained by the re-dissolution of polyimide powders in THF and then precipitation with the solution of methanol/water. The amorphous phase endows the polyimides with good solubility in solvents. Also, it is known that the incorporation of a hexafluoroisopropylidene (6F) group into the polymer backbones enhances the polyimide solubility without sacrificing thermal stability. Thus the resulting side-chain NLO polyimides exhibit good solubility in common organic solvents, such as cyclopentanone, THF, DMF, DMSO, NMP, and even acetone at room temperature. The excellent solubility of the polyimides makes them easier for good optical quality thin films preparation by spin-coating, and they also show the potential for further device fabrication.

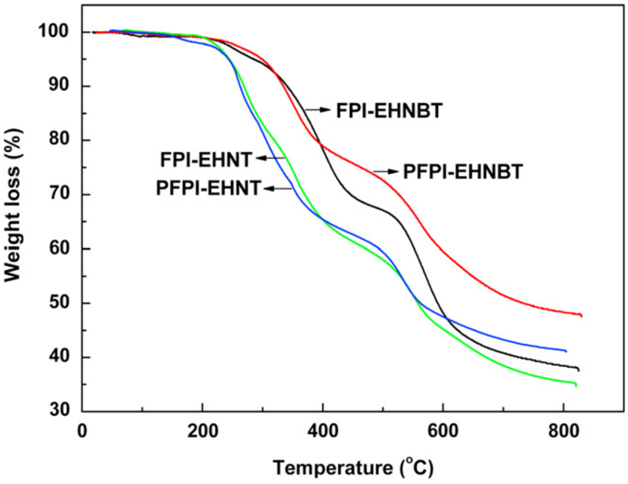

Fig. 4. TGA curves of the side-chain NLO polyimides.

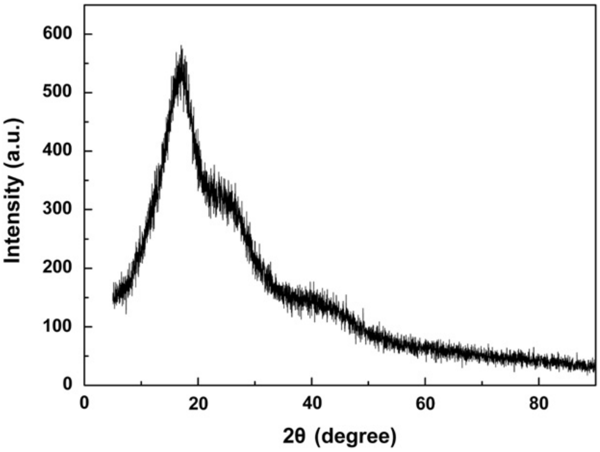

Fig. 5. XRD pattern of polyimide FPI-EHNT.

The polyimides give smooth and physically stable films with thicknesses ranging from 0.2 to 7.0 μm, depending on the spinning speed and the concentration of the solution. The thickness film of the polyimides is listed in Table 2. As shown in Table 2, the values of refractive indexes for the side-chain NLO polyimides investigated are in the range of 1.5597–1.5961. The thermooptic coefficient values of the side-chain NLO polyimides were calculated by linear fit of the refractive indexes at different temperatures at 1550 nm. Fig. 6 shows the variation of refractive index of the side-chain NLO polyimides at TE mode versus temperature. The refractive index of the polymers decreases linearly with increasing temperature, that is to say, the polymers have a negative temperature coefficient of the refractive index. The dn/dT values of FPI-EHNT, FPI-EHNBT,

Table 2
Optical properties of the side-chain NLO polyimides.

	n_{TE}[a]	dn/dT (10^{-4}/°C)[b]	Thickness film (μm)	r_{33} (pm/V)[c]	optical loss (dB/cm)[d]
FPI-EHNT	1.5791	2.008	0.2	20	2.1
FPI-EHNBT	1.5597	1.724	0.3	14	1.9
PFPI-EHNT	1.5961	1.974	6.8	19	2.3
PFPI-EHNBT	1.5821	1.680	7.0	13	2.2

[a] Refractive indices at transverse electric mode measured at 1550 nm.
[b] All values for dn/dT obtained at 1550 nm.
[c] Electro-optic coefficients measured at 1550 nm.
[d] Optical loss measured at 1550 nm.

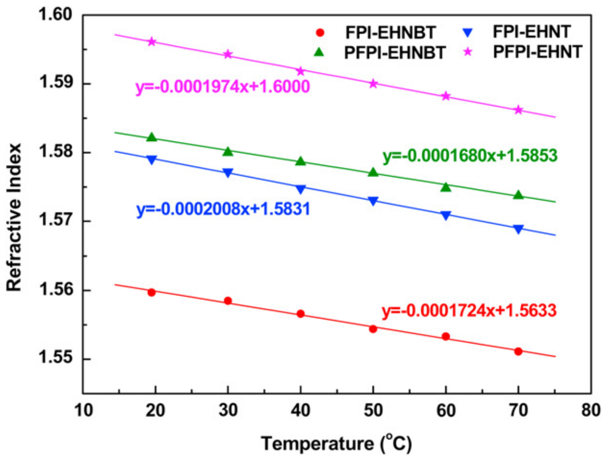

Fig. 6. Refractive index variation of the side-chain NLO polyimides with temperature.

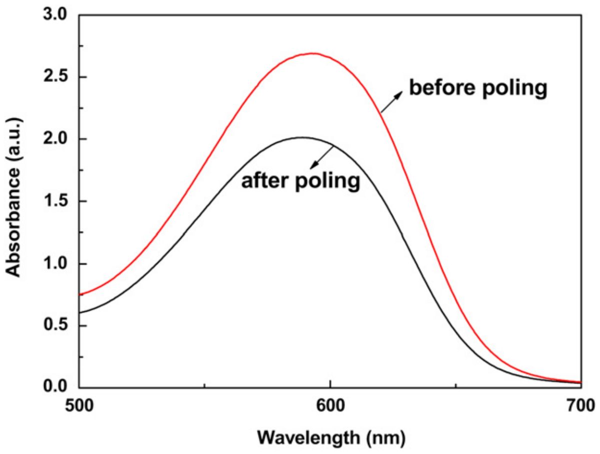

Fig. 7. UV–vis absorption spectra of a film of polyimide FPI-EHNT before and after poling.

PFPI-EHNT and PFPI-EHNBT are -2.008×10^{-4}/°C, -1.724×10^{-4}/°C, -1.974×10^{-4}/°C and -1.680×10^{-4}/°C, respectively, for TE polarization measured at 1550 nm.

The critical issue influencing the utilization of polymeric EO materials is that of optical loss at the communication wavelength. As shown in Table 2, the side-chain NLO polyimides possess low optical losses which are in the range of 1.9–2.3 dB/cm at 1550 nm. Both absorption and scattering of light from materials will contribute to optical loss. For polymer materials, both electronic and vibrational absorptions are likely to result in absorption loss. The absorption maxima of the NLO chromophores are sufficiently far removed from the measurement wavelength that electronic absorptions of the chromophores do not likely contribute to measured loss. In the 1300–1600 nm range, absorptions coming from the overtones of fundamental molecular vibrations are dominant. C–H overtones are highly absorptive in the telecommunication windows, whereas C–F overtones show extremely low absorption throughout the range of interest, owing to their higher harmonic order. Thus fluorine atoms were incorporated into the polyimide matrixes to decrease the absorption loss of the resulting materials. Therefore, in this work, we focus on manipulation of materials composition and processing conditions to reduce scattering loss generated during material processing. There are numerous factors accounting for scattering loss in optical materials. Extrinsic scattering in polymers can originate from dust, unreacted monomer, unfiltered particles, and dissolved bubbles. In order to decrease extrinsic scattering, the polymer solution was filtered through a 0.5 μm syringe filter, and the whole spin-coating procedure was carried out in an ultraclean room. Intrinsic scattering results from density fluctuations and compositional inhomogeneities. The test results show that the uniformity of the film thickness gets better and better with the increase of spinning speed. Thus through controlling the spinning speed we can achieve perfect film thickness uniformity. In addition both amorphous structure of the polyimides and incorporation of hexafluoroisopropylidene groups supply the polymers with good solubility, therefore resulting in flat, smooth and homogeneous optical quality films to be obtained. The homogeneity in the film decreases the scattering of incident light, thus reducing scattering loss.

3.4. Non-linear optical properties

To evaluate the NLO activity of the side-chain NLO polyimides, uniform and transparent thin films were prepared by spinning their cyclopentanone solution onto ITO glass. The noncentrosymmetric alignment of chromophores was achieved by corona poling process. Fig. 7 shows the UV–vis absorption spectra of FPI-EHNT film before and after poling. After the electric poling, the dipole moments of the NLO chromophores were aligned along the direction of the poling field and the UV–vis spectrum of polyimide FPI-EHNT exhibited a decrease in absorption. For the NLO polyimides, the decomposition temperatures of the chromophores are well above the poling one. Thus the decrease in absorbance after poling is an indicator of the dipole alignment and irrelevant to chromophore degradation. The order parameter describes the chromophore alignment and correlates to the NLO properties of the polymer [34]. The order parameter value is zero in a completely disordered system and unity in a system in which all chromophores have their dipole axes along the same direction. From the absorbance change, the order parameter of the poled film could be estimated, being related to the poling efficiency. The estimated order parameter value for FPI-EHNT ($\Phi = 1 - A_1/A_0$, A_0 and A_1 are the absorbances of the polymer film before and after corona poling) was 0.24, showing good poling efficiency. During the corona poling process, the chromophores reorient in the polymer so that their dipole moments is along the field direction which is parallel to the incident light, resulting in the reduction of the peak absorbance of the incident light perpendicular to the film [34,35]. Similarly according to the absorbance change, the order parameter values for FPI-EHNBT, PFPI-EHNT and PFPI-EHNBT were estimated to be 0.25, 0.23 and 0.23, respectively.

The electro-optic coefficients of the side-chain NLO polyimides, measured by a simple reflection method, are listed in Table 2. The side-chain NLO polyimides containing hetarylazo chromophores achieve a high electro-optic coefficient. Relatively high r_{33} values for the NLO polyimides can be ascribed to the large molecular hyperpolarizabilities of hetarylazo chromophores EHNBT and EHNT. The chromophores have a nitrothiazole or a nitrobenzothiazole acceptor group and a substituted amino-benzene donor group linked by a conjugated system containing one azo-bridge. Since the delocalization energy of heteroaromatics, such as benzothiazole or thiazole, is lower than that of benzene, they can offer better conjugation than benzene in donor–acceptor compounds. Moreover the electron-poor benzothiazole and thiazole, which are substituted by an electron-withdrawing NO_2 group increase the acceptor ability of the nitro group and act as auxiliary acceptors. Thus heteroaromatic rings presence in push–pull chromophores is expected to result in enhanced charge-transfer properties and molecular hyperpolarizabilities, in comparison with related systems containing benzenoid rings. And the large molecular hyperpolarizabilities of

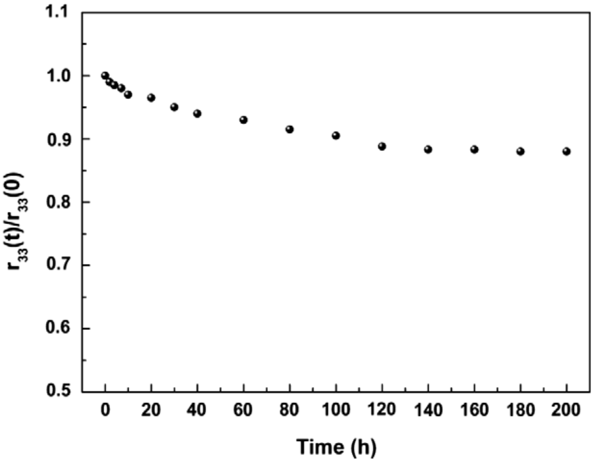

Fig. 8. Temporal stability of the EO coefficient for the poled polyimide FPI-EHNT at 110 °C.

hetarylazo chromophores contribute to high non-linear responses for the NLO polyimides.

The long-term stability of the non-linear property at elevated temperatures is very important for the practical use of NLO polymers. After the poling electric field was turned off, the NLO chromophores, in a sufficiently large local free volume, were free to rotate out of their poling-imposed alignment, causing a fast decay of the EO coefficient. The EO coefficient decay increases with temperature because the local free volume in the polymer enhances with temperature. And this permits the NLO chromophores to rotate quickly into a disordered arrangement, resulting in a rapid decay in the EO coefficient. Fig. 8 shows the temporal stability of EO coefficient for the poled polyimide FPI-EHNT at 110 °C. The r_{33} of FPI-EHNT is stabilized at approximately 88% of its original value at 110 °C for more than 200 h. At room temperature, the temporal stability of the EO coefficient of FPI-EHNT remained about 96% of its initial value, even after two months. These results overcome the relaxation problem in poled NLO polymeric systems. Generally at temperatures close to the glass transition the relaxation of the side-chain chromophores is related to the mobility of the polymeric matrix. However it is believed that at temperatures below T_g, decay of the EO coefficient is strongly dependent on the local mobility of the chromophore instead of the chain segmental motion [36]. Because low temperatures limit motion of the polymer chain to such an extent that local motion of the NLO chromophores become the most important relaxation process. For the side-chain polyimides, because the chromophores are covalently bound to the main chains of the polyimides, at temperatures below T_g the local motions of the chromophores are restricted, thus reducing orientation relaxation [37]. Moreover the heteroaromatic chromophores have a stronger interaction between chromophores, restricting the local motions of the chromophores and reducing orientation relaxation [36]. Therefore polyimide FPI-EHNT exhibit good temporal stability at elevated temperatures. These results demonstrate that the side-chain NLO polyimides posses a high and stable non-linear optical response, even at elevated temperatures. Therefore such polymers can be useful in the field of electro-optics and photonics.

4. Conclusion

Highly electro-optic active thiazole and benzothiazole based chromophores were incorporated into the polymer backbones to prepare a series of novel NLO side-chain fluorinated polyimides via a Mitsunobu reaction. The large molecular hyperpolarizabilities of hetarylazo chromophores contribute to high electro-optic coefficients (as high as 20 pm/V at 1.55 μm) for the NLO polyimides. The polyimides possess high glass transition temperature (T_g) in the range from 193 to 200 °C which result in a stable NLO response at elevated temperature. The polyimides exhibit good organosolubility and excellent film-forming properties due to amorphous structure of the polymers and the introduction of hexafluoroisopropylidene groups. And low optical losses (1.9–2.3 dB/cm at 1.55 μm) were obtained for these polymers by optimum manipulation of film making process. Such new NLO fluorinated polyimides are distinguished by an excellent combination of NLO activity, temporal stability, and optical loss. Moreover the fabrication of EO modulators with the NLO polyimides as the EO materials is in progress.

Acknowledgments

The authors are grateful to Technology Support Program of Jiangsu Province of China (BE2008129) and the National Nature Science Foundation of China (50873026) for financial supports.

References

[1] Jeng RJ, Chang CC, Chen CP, Chen CT, Su WC. Thermally stable crosslinked NLO materials based on maleimides. Polymer 2003;44:143–55.
[2] Luo JD, Haller M, Li HX, Tang H-Z, Jen AK-Y, Jakka K, et al. A side-chain dendronized nonlinear optical polyimide with large and thermally stable electrooptic activity. Macromolecules 2004;37:248–50.
[3] Lindsay GA, Guenthner AJ, Wright ME, Sanghadasa M, Ashley PR. Multi-month thermal aging of electro-optic polymer waveguides: synthesis, fabrication, and relaxation modeling. Polymer 2007;48:6605–16.
[4] Song NH, Men LQ, Gao JP, Bai YW, Beaudin AMR, Yu GM, et al. Cross-linkable zwitterionic polyimides with high electrooptic coefficients at telecommunication wavelengths. Chemistry of Materials 2004;16:3708–13.
[5] Chang H-L, Lin H-L, Wang Y-C, Dai SA, Su W-C, Jeng R-J. Thermally stable NLO poly(amide-imide)s via sequential self-repetitive reaction. Polymer 2007;48:2046–55.
[6] Ju HK, Lim JS, Yoon SC, Lee C, Choi DH, Park SK, et al. Synthesis and optical nonlinearity of thermally stable polyimides incorporated with electro-optic chromophore as side chain. Macromolecular Symposia 2007;249–250:21–8.
[7] Do JY, Park SK, Ju J-J, Park S, Lee M-H. Nonlinear optical polyimides with various substituents on chromophores: synthesis and glass transition temperature. Optical Materials 2004;26:223–9.
[8] Do JY, Park SK, Ju J-J, Park S, Lee M-H. Electro-optic materials: hyperbranched chromophores attached linear polyimide and dendritic polyesters. Polymers for Advanced Technologies 2005;16:221–6.
[9] Saadeh H, Wang LM, Yu LP. A new synthetic approach to novel polymers exhibiting large electrooptic coefficients and high thermal stability. Macromolecules 2000;33:1570–6.
[10] Chao TY, Chang HL, Su WC, Wu JY, Jeng RJ. Nonlinear optical polyimide/montmorillonite nanocomposites consisting of azobenzene dyes. Dyes and Pigments 2008;77:515–24.
[11] Chen T-A, Jen AK-Y, Cai YM. Facile approach to nonlinear optical side-chain aromatic polyimides with large second-order nonlinearity and thermal stability. Journal of the American Chemical Society 1995;117:7295–6.
[12] Chen T-A, Jen AK-Y, Cai YM. Two-step synthesis of side-chain aromatic polyimides for second-order nonlinear optics. Macromolecules 1996;29:535–9.
[13] Becker MW, Sapochak LS, Ghosen R, Xu C, Dalton LR, Shi Y, et al. Large and stable nonlinear optical effects observed for a polyimide covalently incorporating a nonlinear optical chromophore. Chemistry of Materials 1994;6:104–6.
[14] Jen AK-Y, Liu Y-J, Cai Y, Rao VP, Dalton LR. Design and synthesis of thermally stable side-chain polyimides for second-order nonlinear optical applications. Journal of the Chemical Society Chemical Communications 1994:2711–2.
[15] Lee H-J, Lee M-H, Han SG, Kim H-Y, Ahn J-H, Lee E-M, et al. Synthesis and properties of nonlinear optical side chain soluble polyimides for photonics applications. Journal of Polymer Science Part A: Polymer Chemistry 1998;36:301–7.
[16] Van den Broeck K, Verbiest T, Van Beylen M, Persoons A, Samyn C. Synthesis and nonlinear optical properties of high glass transition polyimides. Macromolecular Chemistry and Physics 1999;200:2629–35.
[17] Van den Broeck K, Verbiest T, Degryse J, Van Beylen M, Persoons A, Samyn C. High glass transition chromophore functionalised polyimides for second-order nonlinear optical applications. Polymer 2001;42:3315–22.
[18] Saadeh H, Gharavi A, Yu D, Yu LP. Polyimides with a diazo chromophore exhibiting high thermal stability and large electrooptic coefficients. Macromolecules 1997;30:5403–7.

[19] Miller RD, Burland DM, Jurich M, Lee VY, Moylan CR, Thackara JI, et al. Donor-embedded nonlinear optical side chain polyimides containing no flexible tether: materials of exceptional thermal stability for electrooptic applications. Macromolecules 1995;28:4970–4.

[20] Yang S, Peng Z, Yu L. Functionalized polyimides exhibiting large and stable second-order optical nonlinearity. Macromolecules 1994;27:5858–62.

[21] Yu D, Yu L. Design and synthesis of functionalized polyimides for second-order nonlinear optics. Macromolecules 1994;27:6718–21.

[22] Yu D, Gharavi A, Yu L. A generic approach to functionalizing aromatic polyimides for second-order nonlinear optics. Macromolecules 1995;28:784–6.

[23] Leng WN, Zhou YM, Xu QH, Liu JZ. Synthesis of nonlinear optical side-chain soluble polyimides for electron-optic applications. Polymer 2001;42:7749–54.

[24] Cojocariu C, Rochon P. Synthesis and optical storage properties of a novel polymethacrylate with benzothiazole azo chromophore in the side chain. Journal of Materials Chemistry 2004;14:2909–16.

[25] Qiu L, Shen YQ, Hao JM, Zhai JF, Zu FH, Zhang T. Study on novel second-order NLO azo-based chromophores containing strong electron-withdrawing groups and different conjugated bridges. Journal of Materials Science 2004;39:2335–40.

[26] Chen LJ, Cui YJ, Qian GD, Wang MQ. Synthesis and spectroscopic characterization of an alkoxysilane dye containing azo-benzothiazole chromophore for nonlinear optical applications. Dyes and Pigments 2007;73:338–43.

[27] Benková Z, Černušák I, Zahradník P. Basis set and electron correlation effects on static electric properties of 1,3-thiazoles and 1,3-benzothiazoles as potential fragments in push–pull NLO chromophores. Molecular Physics 2006;104:2011–26.

[28] Batista RMF, Costa SPG, Malheiro EL, Belsley M, Raposo MMM. Synthesis and characterization of new thienylpyrrolylbenzothiazoles as efficient and thermally stable nonlinear optical chromophores. Tetrahedron 2007;63:4258–65.

[29] Razus AC, Birzan L, Surugiu NM, Corbu AC, Chiraleu F. Syntheses of azulen-1-yl-benzothiazol-2-yl diazenes. Dyes and Pigments 2007;74:26–33.

[30] Benková Z, Černušák I, Zahradník P. Theoretical study of static electric properties of benzothiazole containing push–pull systems as potential candidates for NLO materials. Structural Chemistry 2006;17:287–300.

[31] He M, Zhou YM, Liu R, Dai J, Cui YP, Zhang T. Novel nonlinearity-transparency-thermal stability trade-off of thiazolylazopyrimidine chromophores for nonlinear optical application. Dyes and Pigments 2009;80:6–10.

[32] Zhong AM, Zhou YM, Qiu FX. Synthesis and characterization of thiazole chromophores with high second-order polarizability. Acta Chimica Sinica 2006;64:343–7.

[33] Pu H, Liu L, Jiang W, Li X, Chen J. Synthesis and characterization of styrene/maleimide copolymer with 4-[N-ethyl-N-(2-hydroxyethyl) amino]-4'-nitroazobenzene as side chain. Journal of Applied Polymer Science 2008;108:1378–84.

[34] Lu J, Yin J. Synthesis and characterization of photocrosslinkable, side-chain, second-order nonlinear optical poly(ester imide)s with great film-forming ability and long-term dipole orientation stability. Journal of Polymer Science Part A: Polymer Chemistry 2003;41:303–12.

[35] Casalboni M, Caruso U, De Maria A, Fusco M, Panunzi B, Quatela A, et al. New polyurethanes and polyesters for second-order nonlinear optical applications. Journal of Polymer Science Part A: Polymer Chemistry 2004;42:3013–22.

[36] Wang X, Yang K, Kumar J, Tripathy SK, Chittibabu KG, Li L, et al. Heteroaromatic chromophore functionalized epoxy-based nonlinear optical polymers. Macromolecules 1998;31:4126–34.

[37] Döbler M, Weder C, Ahumada O, Neuenschwander P, Suter UW. Main-chain nonlinear optical polymers with enhanced orientational stability. Macromolecules 1998;31:7676–81.